



# Extracellular vesicles of multiple myeloma cells utilize the proteasome inhibitor mechanism to moderate endothelial angiogenesis

Moran Zarfati<sup>1</sup> · Irit Avivi<sup>1,2</sup> · Benjamin Brenner<sup>1,2</sup> · Tami Katz<sup>1,2</sup> · Anat Aharon<sup>1,2</sup>

Received: 12 June 2018 / Accepted: 19 September 2018 / Published online: 1 November 2018  
© Springer Nature B.V. 2018

## Abstract

Bone marrow microenvironment is known to support angiogenesis, thus contributing to progression of multiple myeloma (MM). Bortezomib, a proteasome inhibitor (PI) widely used in MM treatment, has anti-angiogenic activity. Extracellular vesicles (EVs), shedding from cell surface, serve as mediators in cell-to-cell communication. We have hypothesized that MM cells (MMCs) treated with bortezomib generate EVs that could diminish angiogenesis, thus limiting MM progression. In the present study, EVs were obtained from MMCs (RPMI-8226), untreated (naïve) or pre-treated with bortezomib. EVs were outlined using NanoSight, FACS, protein arrays and proteasome activity assays. The impact of MMC-EVs on endothelial cell (EC) functions was assessed, employing XTT assay, Boyden chamber and Western blot. A high apoptosis level (annexin V binding  $70.25 \pm 16.37\%$ ) was observed in MMCs following exposure to bortezomib. Compared to naïve EVs, a large proportion of bortezomib-induced EVs (Bi-EVs) were bigger in size ( $> 300$  nm), with higher levels of annexin V binding ( $p=0.0043$ ). They also differed in content, presenting with increased levels of pro-inflammatory proteins, reduced levels of pro-angiogenic growth factors (VEGFA, PDGF-BB, angiogenin), and displayed lower proteasome activity. Naïve EVs were found to promote EC migration and proliferation via ERK1/2 and JNK1/2/3 phosphorylation, whereas Bi-EVs inhibited these functions. Moreover, Bi-EVs appeared to reduce EC proteasome activity. EVs released from apoptotic MMCs following treatment with bortezomib can promote angiogenesis suppression by decreasing proliferation and migration of EC. These activities are found to be mediated by specific signal transduction pathways.

**Keywords** Multiple myeloma (MM) · Extracellular vesicles (EVs) · Proteasome inhibitor (PI) · Endothelial cells (EC) · Angiogenesis

## Introduction

Bone marrow (BM) microenvironment is known to produce and secrete cytokines and growth factors, inducing angiogenesis [1] that in its turn supports proliferation and survival

of malignant cells in multiple myeloma (MM) [2–4]. Increased BM angiogenesis, termed the angiogenic switch [5], has been found to be associated with cell transformation from the pre-angiogenic stage of slow tumor progression to the leukemic stage [4]. Since enhanced BM neovascularization corresponds to a worse outcome [6], its suppression could be crucial for the control of MM progression.

Interaction between the vascular endothelial growth factor (VEGF) and its receptor (VEGF-R) on the endothelial cells (ECs) is established to be the main pathway to induce angiogenesis signaling [7]. The use of VEGF-R blockers is reported to limit EC proliferation, thereby restricting MM cell (MMC) growth and migration [8].

The ubiquitin–proteasome pathway of protein degradation is involved in the regulation of the cell cycle and repair of DNA damage [9]. Treatment of MM with proteasome inhibitor bortezomib is reported to diminish the function of proteasome catalytic sites. Specifically, bortezomib affects

Tami Katz and Anat Aharon equally contributed to this study.

**Electronic supplementary material** The online version of this article (<https://doi.org/10.1007/s10456-018-9649-y>) contains supplementary material, which is available to authorized users.

✉ Anat Aharon  
a\_aharon@yahoo.com

<sup>1</sup> Bruce Rappaport Faculty of Medicine, Technion, Israel Institute of Technology, Haifa, Israel

<sup>2</sup> Department of Hematology and Bone Marrow Transplantation, Rambam Health Care Campus, 7, Ha'Aliya St., Haifa 3109601, Israel

MMCs through the suppression of NF- $\kappa$ B signaling pathway, resulting in the down-regulation of anti-apoptotic target genes [10], and massive cell apoptosis [11]. This also leads to inhibition of cytokine secretion, angiogenesis and MMC adhesion to BM microenvironment [12].

Extracellular vesicles (EV), including exosomes, micro-particles, and apoptotic bodies [13], have been established to play a key role in the intercellular communication [14]. By transferring their cargo of regulatory molecules, EVs can modulate angiogenesis, thus promoting tumor development, progression, and metastasis [15–17].

EVs originating from various types of malignant cells (those of hematological and solid tumors) display a unique profile, including specific membrane antigens, cytokine content, DNA fragments, and miRNA [18]. We have recently demonstrated that patient EVs released from BM acute myeloid leukemia (AML) cells are characterized by a high expression of CD117 and CD34, and increased cytokine content, which decreases following chemotherapy treatment [19]. Moreover, in another study of ours, chemotherapy administration to breast cancer patients has been found to affect the EV profile and function [20].

Stimulation of both MMCs and ECs by naïve MMC-derived EVs was previously reported to result in increased proliferation and migration of these cells [21, 22]. However, the mechanism related to the effect of EVs generated from MMCs—following exposure to chemotherapy, such as a proteasome inhibitor, on angiogenesis has not been elucidated.

We have hypothesized that EVs secreted from MMCs are involved in angiogenesis and disease progression, while treatment of myeloma cells with bortezomib could change properties of the generated EVs, resulting in suppression of their pro-angiogenic activities.

## Materials and methods

### Cell culture and EV isolation

MM cell line RPMI 8226 (ATCC) was cultured in RPMI 1640 medium supplemented with 10% heat-inactivated fetal calf serum (FCS), 1% L-glutamine, 1% Antibiotics Solution (10,000 units/ml penicillin, 10 mg/ml streptomycin, 250 units/ml nystatin; all purchased from Biological Industries, Beit Haemek, Israel). For EV isolation, the cells were either untreated or treated with 100 nM of bortezomib, as a single dose, for 24 h in fresh growth medium supplemented with 10% FCS. In an attempt to maximize the effects of bortezomib, the drug dose of 100 nM was chosen. This concentration was previously used in other studies, demonstrating growth inhibition and apoptosis of human MMCs, the effects required from an anti-myeloma drug [23]. The medium was then collected and centrifuged for 15 min at

1500 $\times$ g. Supernatant was further centrifuged twice for 1 h at 20,000 $\times$ g followed by washing. An EV pellet was then frozen in aliquots at  $-80^{\circ}\text{C}$ .

Human umbilical vein endothelial cells (HUVEC) were isolated from human umbilical cord veins obtained from four healthy pregnant women after delivery at term, according to the previously described technique [24, 25]. Based on the approach described by Liao H. et al. and according to our experience, HUVEC at passages 3–8 were used for testing cell functions [26]. These cells were seeded in 24-well plates pre-coated with fibronectin (Biological Industries, Beit Haemek, Israel) or in flasks with M199 medium supplemented with 18% FCS, 1% Antibiotics Solution, 0.01% Amphotericin B (Sigma-Aldrich, MO), 3.3 U/ml heparin (Bondene Pty, South Africa), and 25 mg/ml endothelial mitogen (Biomedical technologies, MA) at  $37^{\circ}\text{C}$  and 5%  $\text{CO}_2$ . Before exposure to EVs, the HUVEC medium was replaced with medium-free serum or with PBS in case when the effect of EVs on EC proliferation was validated.

The Mvt-1 mammary cancer cell line was used as a positive control for p-MAPKAPK-2 phosphorylation.

### EV quantification

The EV size and concentration were determined using NanoSight NS300 Analyzer (NanoSight, UK), measuring particles of 30–1000 nm, and flow cytometer—CyAn ADP analyzer (Beckman Coulter, Switzerland) measuring EVs  $>300$  nm. For flow cytometry experiments, EVs were evaluated using 0.75 micron beads and EV concentration was measured using 7.58  $\mu\text{m}$  beads as described previously [27]. Briefly, 7.58- $\mu\text{m}$  count beads (Flow Cytometer Absolute Count Standard, Bangs Laboratories Inc., IN, USA) and 50  $\mu\text{l}$  of EVs samples were combined and the total number of EVs per 1 ml in the EV gate area was calculated accordingly.

### MMC and MMC-EV characterization

MMCs and EVs were characterized using annexin V-FITC/propidium iodide apoptosis kit (Bender MedSystem, Vienna, Austria) and conjugated mouse anti-human antibodies: PE-syndecan-1/CD138 and APC-CD38, PE-IgG 1 k Isotype control, APC-Flt-1 (vascular endothelial growth factor receptor—VEGF-R1), PE-KDR (vascular endothelial growth factor receptor—VEGF-R2), APC-IgG 1 k Isotype control (R&D Systems, MN).

MMCs and their derived EVs were stained with conjugated antibodies for 15–30 min at room temperature. Samples were fixed with 0.5% formaldehyde. Cell acquisition was evaluated by flow cytometry (Cytex flow Cytometry product Merckel, Israel) and analyzed by FlowJo software 7.6.4. (Tree Star Inc, Oregon). EV acquisition was assessed by flow cytometry, CyAn ADP analyzer

(Beckman Coulter, Switzerland) and the analysis was performed using Summit 4.3 software (Dako, Denmark). Results were expressed as the proportion (%) of positively labeled cells/EVs for a particular antigen.

### EV protein content

EVs were isolated as previously described and re-suspended in lysis buffer with protease inhibitors (RayBiotech, Inc., GA). Using a quantification kit (BCA protein, quantification kit, Thermo Fisher Scientific Inc., Waltham, MA), 100 µg of total protein obtained from MMC-EVs was loaded to a glass chip angiogenesis antibody array (RayBiotech, Inc., GA) according to manufacturer's instruction. Fluorescence intensity was analyzed using a microarray scanner (Molecular Devices, CA) and its software, which calculated the mean intensity of each spot minus background and the negative control. The results were normalized to positive control spots, and a controlled amount of biotinylated IgG antibody was printed directly onto the glass surface. Changes in the signal intensity for a single analysis between samples were measured by any  $\geq$  twofold increase or  $\leq$  0.5-fold decrease.

### MMC-EVs and endothelial cells interaction

MMCs were incubated with 2 µM Calcein-AM, a green fluorescent cell marker, for 45 min at 37 °C. Following this procedure, cells were stimulated with 10 µM Calcium ionophore A23187 (Sigma-Aldrich) for 15 min in room temperature for intense shedding of EVs. Fluorescent EVs were isolated and co-incubated with non-fluorescent HUVEC for 30 min at 37 °C. The interaction between EVs and HUVEC was measured by an ImageStream-Amnis flow cytometry. The cell fluorescent intensity on the membrane (negative signal) and in the cytosol area (positive signal) reflected the rate of EVs binding to cell membrane or their internalization to the cell (penetration to the cells through the cell membrane).

### EC proliferation assay

HUVEC were seeded in 96-well tissue culture plates in growth medium. After 24 h, the medium was replaced by PBS with or without 50 µg of EVs derived from either naïve MMCs (RPMI 8226 cell line) or those pre-treated with 100 nM of bortezomib. Following 16 h, 50 µl of XTT reaction solution [2,3-bis(2-methoxy-4-nitro-5-sulfophenyl)-2H-tetrazolium-5-carboxanilide] (Biological Industries, Beit Haemek, Israel) were added for 30 min. The absorbance of the samples was measured using ELISA reader 450/630 nm.

### EC migration assay

EVs (50 µg), obtained from naïve MMCs or those pre-treated with bortezomib (100 nM), in a 600 µl serum-free medium, were added to the lower compartment of the Boyden chamber (BD Biosciences; Pharmingen, CA), while HUVEC ( $7 \times 10^4$  cells/100 µl) were seeded in a serum-free medium on the upper chamber membrane. After 24 h of stimulation, inserts were fixed with 4% formaldehyde (FA) in PBS and stained with 0.5% crystal violet (Sigma-Aldrich, MO) for 10 min. Cells from the upper side of the membrane were removed and cells that migrated to the underside of the membrane were photographed using inverted microscope. Images were analyzed for confluence using image J software (National Institutes of Health, USA).

To examine the ability of MMC-EVs to promote HUVEC migration and phosphorylation, in some experiments, HUVEC were pre-exposed for 1 h to specific inhibitors of cell signal transduction, including U0126 (MEK 1/2 inhibitor), PD98059 (MEK1 inhibitor) SP600125 (JNK-1,-2,-3 inhibitor), and SB203580 (p38 inhibitor) (Cayman Chemical Company, MI).

### Protein extraction and western blot analysis

The expression of ERK1/2, c-Jun, and MAPKAPK-2 was assessed by Western blotting. Following overnight starvation HUVEC were stimulated for 24 h with 300 µg/ml of MMC-EVs.

HUVEC were washed twice with PBS and dissolved in the radio-immunoprecipitation assay (RIPA), a protein lysis (Merck Millipore, Germany) with a cocktail of protease and phosphatase inhibitors (Sigma-Aldrich, Israel). Following incubation on ice for 30 min and centrifugation, the supernatants were collected and the protein concentrations were determined (BCA protein, quantification kit). Proteins were electrophoresed through a 10% polyacrylamide gel and transferred to a nitrocellulose membrane (Bio-Rad, Richmond, CA) by electroblotting. Membranes were blocked overnight at 4 °C and immunoblotted with the desired antibody, followed by secondary antibody conjugated with horseradish peroxidase (HRP). The following antibodies against mitogen-activated protein kinases were used: phospho-p44/42<sup>(Thr202/Tyr204)</sup> MAPK, total p44/42-MAPK (Erk1/2), phospho-c-Jun<sup>(Ser73)</sup>, total c-Jun, phospho-MAPKAPK-2<sup>(Thr222)</sup>, total MAPKAPK-2, (Cell Signaling Technology, MA), and  $\beta$ -actin (Sigma-Aldrich, MO). Membranes were developed by enhanced chemiluminescence (ECL) (Biological Industries, Kibutz Beit, Israel) and analyzed using luminescent image analyzer (Fujifilm, Tokyo, Japan). Analysis was performed using Image J software (National Institutes of Health, USA). Positive control for p-MAPKAPK-2 antibody

was executed by testing MAPKAPK-2 phosphorylation of Mvt-1 cells.

### Bortezomib content in EVs

MMC-EVs, obtained from either naïve cells or those pretreated with bortezomib (100 nM), were evaluated for the presence of bortezomib, using high-performance liquid chromatography (HPLC, Agilent 1100 chromatographic system). Bortezomib was separated on C18 column, 20% acetonitrile: 80% water + 0.1% formic acid. Retention time bortezomib = 7.30 min,  $I_{\max}$  = 270 nm, injection volume 60  $\mu$ l. Injection volumes for EVs were 100  $\mu$ l and 300  $\mu$ l. Naïve EVs were used as a control.

### Proteasome activity in EVs and ECs

Proteasome activity in MMC-EVs and ECs was assessed using a proteasome activity kit, (Sigma-Aldrich, Israel) as described previously [28]. Briefly, HUVEC (20,000 cells/well) were seeded in 96-well tissue culture plates in growth medium. Following 2 h, the medium was replaced by fresh medium containing EVs (50  $\mu$ g) obtained from naïve MMCs or treated with bortezomib for 24 h. MMC-EVs (naïve or Bi-EVs) seeded without HUVEC served as control. For evaluation, 100  $\mu$ l of fluorogenic proteasome LLVY-R110 substrate was added to each well for 5 h. Florescence intensity indicated the cleavage of the substrate measured at  $Ex/Em$  = 485/520 (RFU).

### Statistical analysis

Data were analyzed using GraphPad Prism 5 software. Statistical significance was determined using one-way

analysis of variance (ANOVA) followed by Bonferroni's test ( $*p < 0.05$ ,  $**p < 0.01$ ,  $***p < 0.001$ ). *t* test-non-parametric Mann–Whitney test was used for comparing two samples. All data are presented as mean  $\pm$  SD (apart from the pro-angiogenic protein array, a screening test performed only once). Results with a *p* value  $< 0.05$  were considered statistically significant.

## Results

### Bortezomib increased the concentration of large MMC-EVs

The current study evaluated potential effects of bortezomib on the characteristics of Bi-EVs. Two measurement techniques were employed to evaluate the size and concentration of generated EVs.

Nanosight analysis showed that the majority of EVs were smaller than 300 nm, and the mean size of Bi-EVs ( $98 \pm 26$  nm) was lower, albeit non-significantly, than that of naïve EVs ( $113 \pm 11.5$  nm) (Fig. 1a, b). Assessment of total EV concentrations demonstrated a trend of increase in Bi-EVs ( $26.18 \pm 1.47E8$  particles/ $\mu$ l) compared to naïve EVs ( $22.73 \pm 2.71E8$  particles/ $\mu$ l). Of note, the baseline concentration of EVs, as observed in the RPMI medium supplemented with FCS, was found to be  $1.29E7$  particles/ $\mu$ l. Among the Bi-EVs, a threefold higher amount of particles larger than 300 nm was revealed, compared to naïve EVs ( $35.55E3 \pm 29.67E3$  and  $10.74E3 \pm 15.21E3$ , respectively;  $p = 0.0379$ ; Fig. 1c), although the absolute count of such large particles remained less than 1% of the total EV number (defined by Nanosight).

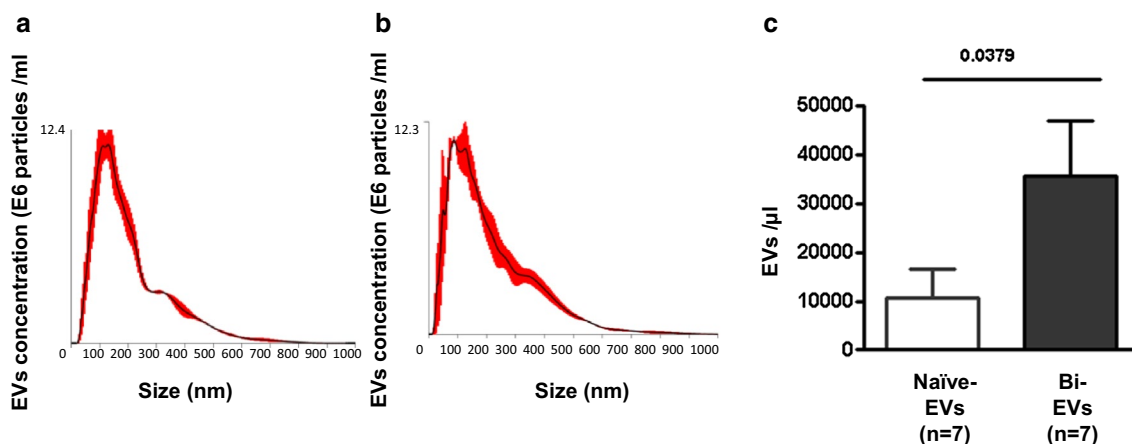


**Fig. 1** MMC EV size and concentration. EVs were isolated from an untreated myeloma cell line (RPMI 8226; naïve MMC-EVs) or following exposure to 100 nM of bortezomib (Bi-EVs). NanoSight

analysis displays size distribution: **a** naïve MMC-EVs; **b** MMC-EVs exposed to 100 nM of bortezomib. Concentrations of large EVs (> 300 nm) were measured by flow cytometry (**c**)

The levels of annexin V binding and propidium iodide (PI) staining, identifying apoptotic cells, were found to be twice higher in bortezomib-treated MMCs, than in naïve MMCs (annexin V:  $70.25 \pm 16.37\%$  vs.  $38.45 \pm 10.1\%$ ,  $p < 0.01$ ; PI staining:  $50.47 \pm 18.56\%$  vs.  $20.98 \pm 10\%$ ,  $p < 0.05$ ). Nevertheless, non-significantly (NS) higher labeling with annexin V was found in Bi-EVs compared with naïve EVs ( $93.73 \pm 18.58\%$  vs.  $73.44 \pm 3.1$ ), and no difference in PI staining ( $17.18 \pm 21.03\%$  vs.  $19.74 \pm 9.26\%$ ) (Fig. 2a, b).

The evaluation of MM markers expression showed that while bortezomib significantly reduced the expression levels of CD38 and CD138 on MMCs (CD38: naïve MMCs  $78.64 \pm 15.75\%$  vs. Bi-MMCs  $56 \pm 16\%$ ,  $p < 0.01$  and CD138: naïve MMCs  $70.81 \pm 15.66\%$  vs. Bi-MMCs  $20 \pm 10\%$ ,  $p < 0.001$ , respectively), non-significant differences were found in the expression level of these markers on

both EV types (CD38: naïve EVs  $28.50 \pm 19.26$  vs. Bi-EVs  $40.79 \pm 23.76$ ; CD138: naïve EVs  $17.83 \pm 11.81$  vs. Bi-EVs  $15.33 \pm 12.29$ ) (Fig. 2c, d).

**Bortezomib altered the levels of pro-angiogenic and inflammatory proteins in MMC-EVs**

As regulation of vasculature requires modulation of angiogenic factors and inhibitors, the EV expression of VEGF-R and content of growth factor molecules were examined. It was found that bortezomib induced a non-significant decrease in the surface expression of VEGF-R1 compared to untreated MMCs (from  $32.1 \pm 5.15\%$  to  $21.12 \pm 7.75\%$ ), while EV levels were found to be similar in both groups, ~30% with broad standard deviation.

At the same time, a trend of reduction was found in the expression of VEGF-R2 on bortezomib-subjected

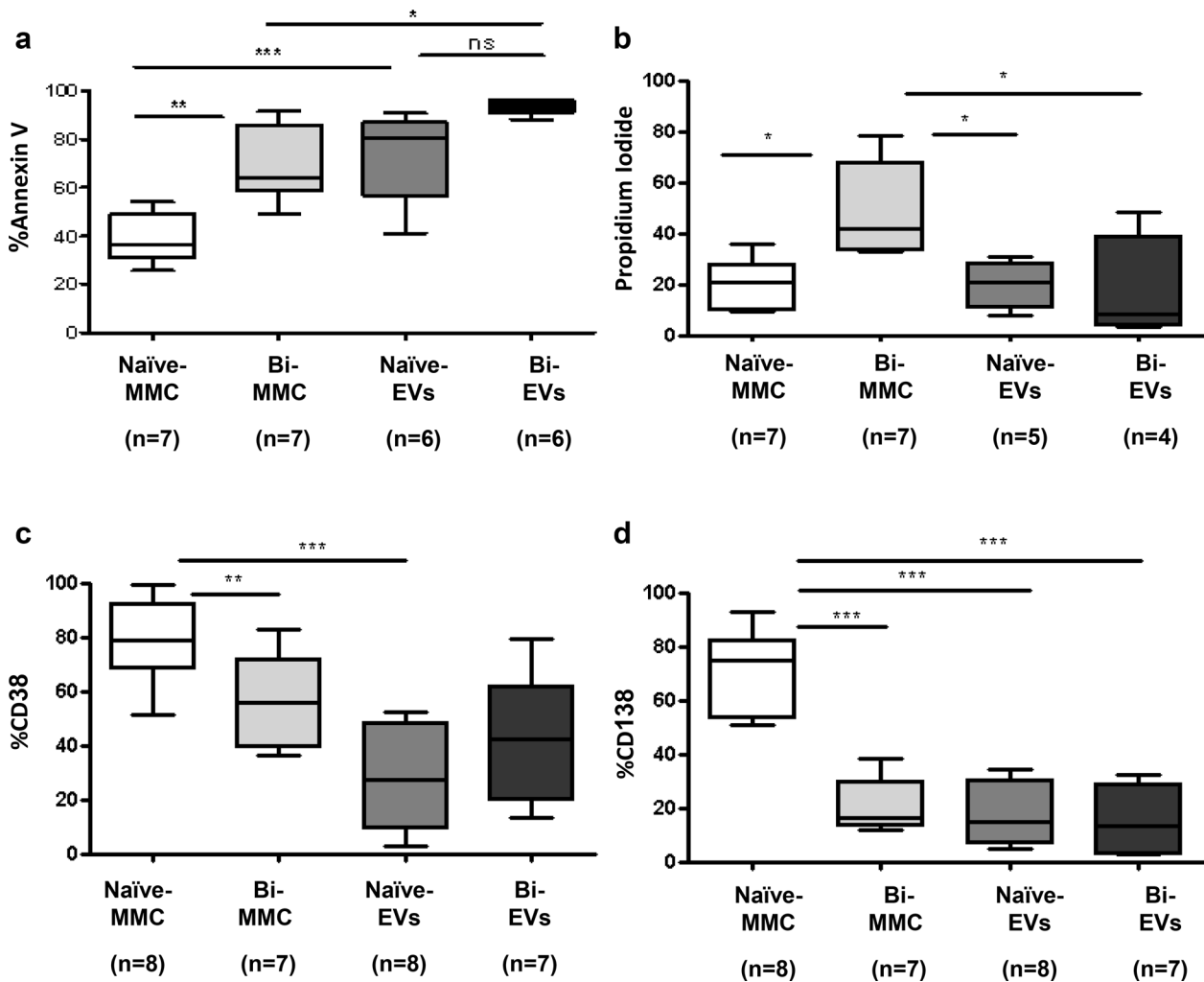


**Fig. 2** Expression of MM markers. EVs were isolated from untreated MMCs (naïve MMC-EVs) or following exposure to 100 nM of bortezomib (Bi-EVs). Cells and their related EVs were stained with

annexin V (a) and propidium iodide (b) or with conjugated antibody against: c CD38 and d CD138 and evaluated by flow cytometry analysis

cells compared to naïve cells (from  $5.268 \pm 2.748\%$  to  $2.62 \pm 2.80\%$ ) and a significant reduction was observed on their related EVs compared to naïve EVs ( $15.84 \pm 2.27\%$  vs.  $29.26 \pm 5.62\%$ ;  $p < 0.001$ ; Fig. 3a). Remarkably, EV VEGF-R2 levels appeared to be significantly higher on EVs compared to their parental cells.

Furthermore, the evaluation of the content of pro-angiogenic proteins derived from naïve EVs revealed high levels of several growth factors: VEGFA, platelet-derived growth factor-BB (PDGF-BB), angiogenin and urokinase plasminogen activator receptor (uPAR). In Bi-EVs, the expression of most of these growth factors was significantly reduced, while the uPAR level appeared to be increased by 2.6 fold. In addition, opposite trends were found in the content of pro-inflammatory cytokines and Bi-EVs demonstrated elevated levels of the interleukins (IL) IL1  $\beta$ , IL-8 IL-10, and chemokine RANTES (regulated on activation, normal T cell expressed and secreted) compared to naïve EVs (Fig. 3b).

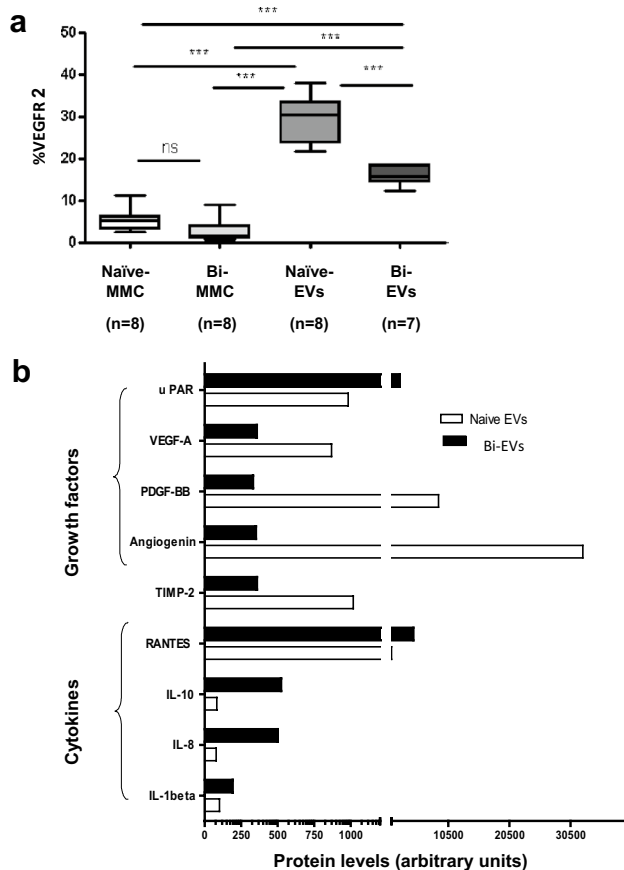


**Fig. 3** The content of membrane angiogenic receptors and proteins in MMCs and EVs. EVs were isolated from an untreated MMC line (naïve MMC-EVs) or following exposure to 100 nM of bortezomib (Bi-EVs): **a** VEGF-R2 and were analyzed by flow cytometry. **b** The protein content of EVs was evaluated using human angiogenesis antibody protein array. The graphs display signal intensity of each protein

## Bi-EVs inhibited proliferation and migration of endothelial cells

Evaluation of the interaction between MMC-EVs and ECs demonstrated 42%-penetration of EVs (reflecting the rate of EV internalization into HUVEC) following co-incubation, as measured by flow cytometry (Fig. 4a1). Fluorescent-labeled naïve EVs which have not been internalized into the cells are represented in Fig. 4a2.

We then examined whether the uptake of MMC-EVs into ECs affected the properties of the latter cells that are considered crucial for angiogenesis. Exposure to naïve EVs induced a trend of increase (30%) in EC proliferation, whereas Bi-EVs inhibited EC proliferation by 50% ( $p < 0.05$ ) (Fig. 4b). A similar pattern of MMC-EV effects on EC migration was revealed. Naïve EVs led to a significant elevation in EC migration (by 13-fold) ( $p < 0.001$ ), while Bi-EVs restricted the migratory effect by 75% ( $p < 0.01$ ), exhibiting the level comparable to that observed in untreated ECs (Fig. 4c).

## MMC-EVs regulated endothelial signal transduction pathways

Given the established role of VEGF/VEGF-R2 signal transduction pathways (ERK, JNK and P38) in EC migration, inhibitors, targeting these signaling pathways, were applied to study the EV effects on EC protein phosphorylation and migration.

HUVEC were found to respond to naïve EVs and displayed a significant increase in ERK1/2 phosphorylation (35 fold,  $p < 0.01$ ; Fig. 5a, S1a) and c-Jun phosphorylation (1.8 fold,  $p < 0.01$ ) (Fig. 5b, S1b), but did not affect MAPKAPK-2 phosphorylation (P38 pathway) (S1c). In contrast, exposure of ECs to Bi-EVs restricted EC ERK1/2, c-Jun and MAPKAPK-2 phosphorylation. The use of signal transduction inhibitors specifically targeting the three MAPK subgroups showed that exposure of HUVEC, pre-treated with MEK1/2 and JNK-1,-2,-3 inhibitors, to naïve EVs significantly reduced ERK1/2 and c-Jun phosphorylation ( $p < 0.05$  and  $p < 0.001$ , respectively) compared stimulation with naïve EVs only.

To further confirm our observations that MMC-EVs activate the MAPK cascade and possibly promote cell migration, we tested HUVEC migration in response to the same signal transduction inhibitors. Co-incubation of HUVEC with both MEK1/2 and JNK-1,-2,-3 inhibitors followed by exposure to naïve EVs was found to diminish the HUVEC migration rate by 80% ( $p < 0.05$ ) and 75% ( $p < 0.5$ ), respectively. Neither MEK1 nor p38 inhibitor had a significant effect on cell migration (Fig. 5c1, c2).

It has been also explored whether the effect of Bi-EVs on ECs is mediated by the drug residues inside EVs that are

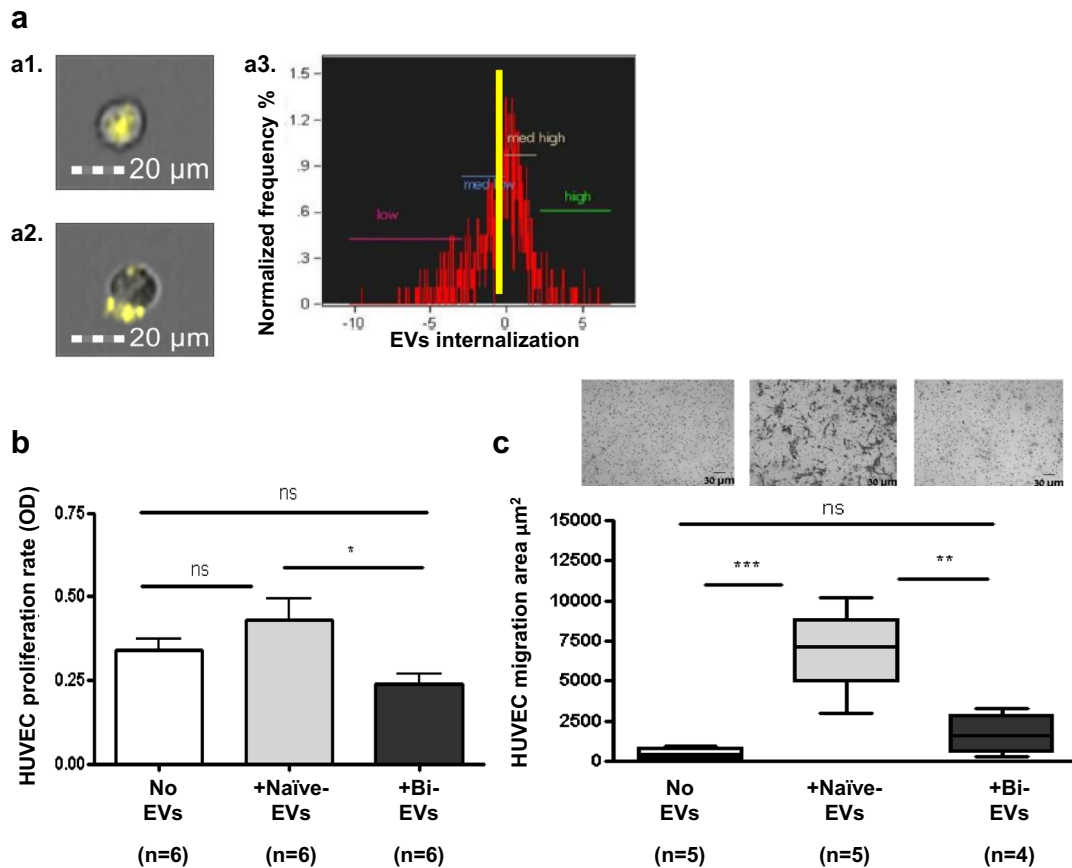


**Fig. 4** MMC-EVs enhance EC proliferation and migration. **a** Fluorescent-labeled naïve EVs were incubated with HUVEC. Fluorescent intensity of the cell membrane (negative signal) and the cytosol area (positive signal) reflected the rate of EV internalization into the cells, as measured by Amnis flow cytometry. **b** To assess proliferation, HUVEC were seeded in 96-well plates (70% confluence) with EVs (50 µg) for 16 h. HUVEC without EVs served as control. Prolifera-

tion rate was measured using the XTT assay. **c** Migration was measured using the Boyden chamber. HUVEC were added to the upper chamber of the insert, while EVs (50 µg) were added to the lower chamber in serum-free medium. Representative light microscope images of cells and the graph display an average area of migrated cells of 10 fields per well. The analysis was executed using Image J software

transported to the cells within the EV cargo or via an active proteasome mechanism present in EVs. The evaluation of bortezomib presence has shown that Bi-EVs have not exhibited any residual molecules of the drug (Fig. 6a). Furthermore, proteasome activity has been found to be decreased (by 60%) in Bi-EVs compared to naïve EVs ( $p = 0.0019$ ) (Fig. 6b1). Likewise, while an addition of naïve EVs to ECs did not affect the EC proteasome activity, it was reduced by 50% in ECs incubated with Bi-EVs ( $p < 0.001$ ) (Fig. 6b2).

### Discussion

There is growing evidence on the role of EVs in intercellular communication associated with cancer progression. Recent studies have demonstrated that MM-derived exosomes modulate the BM microenvironment by enhancing angiogenesis and immunosuppression [29]. It has been shown that cell

exposure to chemotherapeutic drugs results in shedding of modulated EVs, which may change their effects on the recipient cell functions, including angiogenesis [15, 17].

Bortezomib is the first proteasome inhibitor that has become the standard of care in MM [30]. The biologic relevance of proteasome inhibitors in targeting MM cells and the bone marrow microenvironment is well established [23, 31]; however, the potential role of EVs, produced in response to PI exposure has not been explored yet. The current study used high-dose bortezomib (100 nM) for MMC stimulation, which induced cell death (indicated by high annexin V/PI labeling). Such stimulation had been previously reported to cause cell growth inhibition and apoptosis [23]. This setting allowed production of EV amounts sufficient to explore their impact on the angiogenesis process.

Cancer therapy enhances shedding of various EV subpopulations, including exosomes, which are smallest, microvesicles (MVs) and apoptotic bodies. These subpopulations

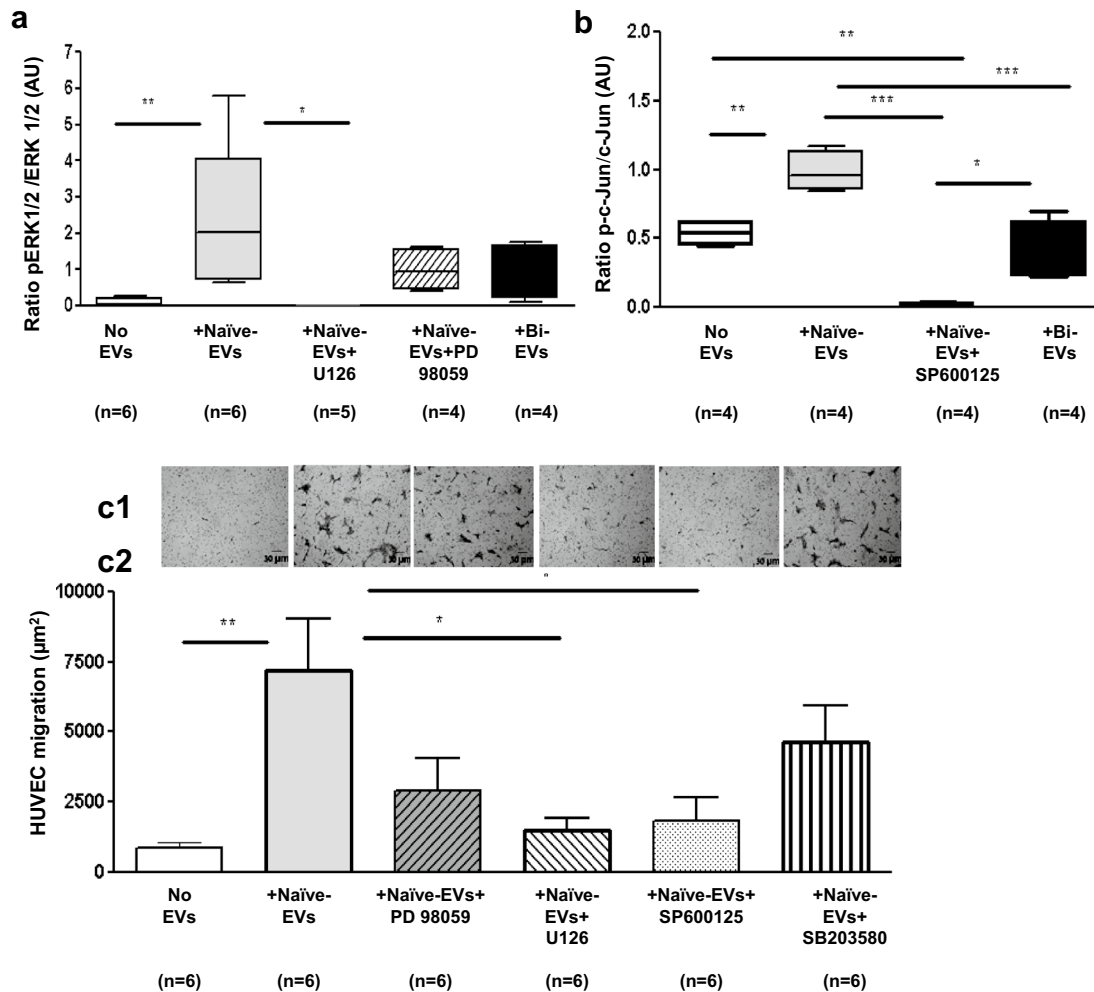


**Fig. 5** Effects of MMC-EVs on EC signaling and proteasome activity. HUVEC were incubated in the serum-free medium for 16 h followed by addition of inhibitors U0126, PD98059, SP600125, and SB203580 for 1 h. EVs generated from the RPMI 8226 cell line (MMC-EVs: naïve MMC-EVs and Bi-EVs) were added to the culture for 15 min. Cellular lysates were separated by SDS-PAGE. Phosphorylation and protein levels of **a** ERK1/2, **b** c-Jun, were assessed using western blot (equal protein loading was confirmed with  $\beta$ -actin). Phosphorylation levels were normalized to the total protein expression and dis-

played in graphs (**a**, **b**). Positive control for p-MAPKAPK-2 antibody was executed by testing MAPKAPK-2 phosphorylation of Mvt-1 mammary cancer cells. For migration, HUVEC treated for 1 h with the above inhibitors were added to the upper chamber of the insert. MMC-EVs in the serum-free medium were added to the lower chamber. Treatment without EVs served as negative control. Representative light microscope images of cells (**c1**) and the graphs (**c2**) display an average area of migrated cells of 10 fields per well. The analysis was executed using Image J software

differ from one another by size, cell origin and function, mechanisms of formation RNA/DNA protein content and surface molecules [32–34]. As MMCs are known to express high levels of membrane MM markers (CD38, CD138) [35], the exposure to bortezomib reduces their expression on MMCs. However, in our study, both MMC-related EV subgroups (naïve-EVs and Bi-EVs) have been found to exhibit low levels of these markers. Of note, the expression of CD38 and 138 is tricky to validate and it may be considered a challenge to perform flow cytometry studies of these markers, especially on EVs.

At least three mechanisms of interaction between EVs and their recipient cells have been reported. They include

endocytosis, EV incorporation with the cell membrane and binding of receptors and antigens [36]. The latter mechanism implies the key role of receptor presentation on the EV surface, which may determine not only the cell/EV binding but also the EV ability to transfer functional receptors to recipient cells [37, 38]. In our study, no significant differences were found in VEGFR-1 (FLT1) expression between MMCs and their EVs, whereas high levels of VEGFR-2 (KDR) were revealed on both naïve and Bi-EVs.

Our results have demonstrated that EVs released from MMCs are internalized into ECs and thus mediate their functioning, e.g., induce migration, proliferation and protein phosphorylation. It can be assumed that by transferring

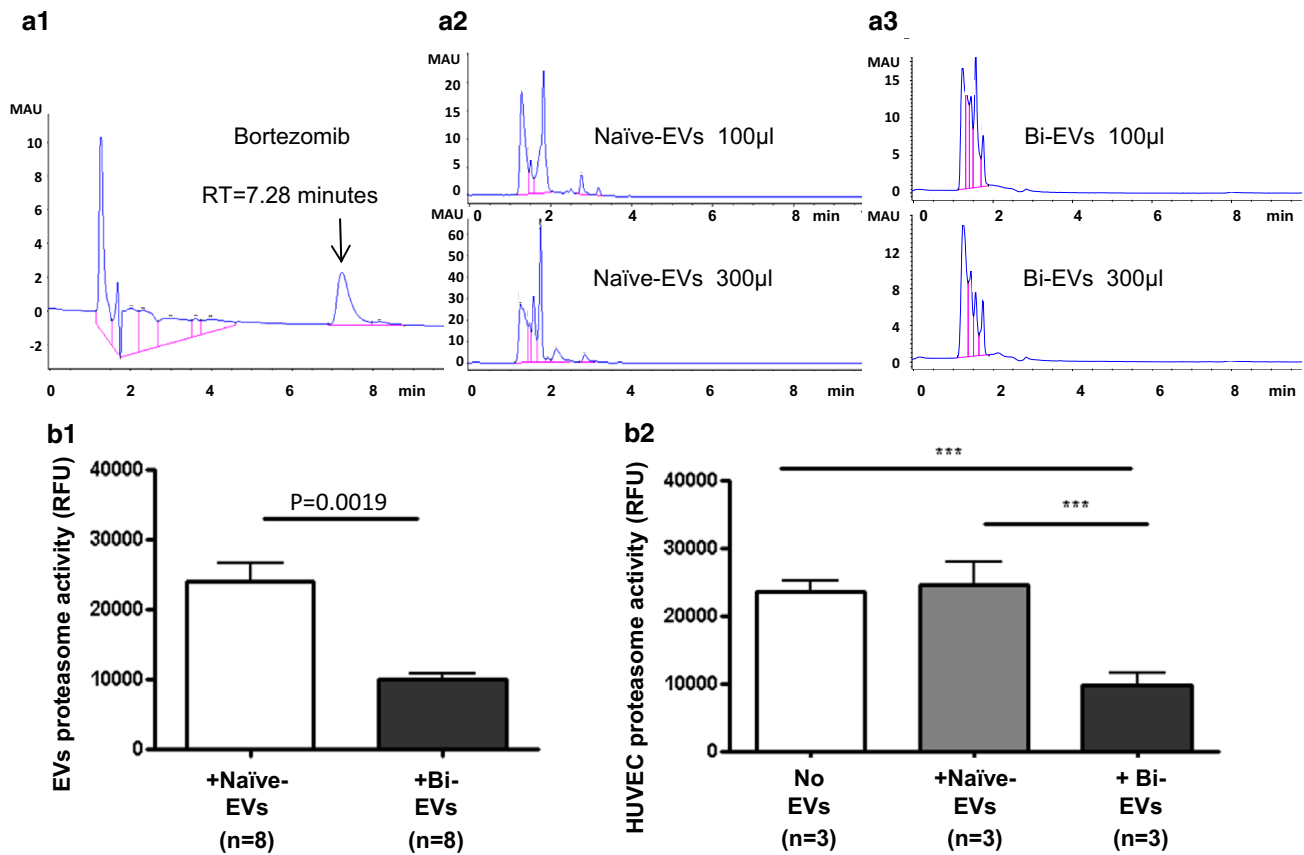


**Fig. 6** MMC-EVs Bortezomib content and proteasome activity in MMC-EVs and EC. **a1–a3** EVs were isolated from untreated MMCs (naïve MMC-EVs) or following exposure to 100 nM of bortezomib (Bi-EVs). The bortezomib content in EVs was determined using HPLC Agilent 1100 chromatographic system. Representative chromatograms of bortezomib (1 µg/ml) (**a1**), naïve MMC-EVs (100 µl and 300 µl) (**a2**), and Bi-EVs (100 µl and 300 µl) (**a3**) are displayed.

**b1, b2** Proteasome activity was assessed, using a proteasome activity kit, in MMC-EVs alone and in HUVEC untreated or treated with MMC-EVs, as described in “Materials and methods.” Fluorescence intensity was measured at the Ex/Em wavelength of 485/520=RFU. **b1** Proteasome activity in MMCs-EV. **b2** Proteasome activity in HUVEC

higher levels of functional VEGFR-2 to ECs, MMC-EVs may enhance the EC angiogenic potential.

The angiogenic switch [5] is essential for MM progression and controlled by a variety of cytokines [39, 40]. The EV membrane shield protects cytokines and growth factors from rapid degradation, enhancing their potential effects [18]. The differences in the expression of pro-angiogenic and anti-angiogenic factors in EVs found in the current study may reflect the imbalance associated with the disease and may indicate the potential ability of EVs to be involved in the angiogenic switch.

Since EVs can influence angiogenesis, their content and surface molecule expressions are of particular importance. The EV cargo is reported to be affected by the stimulus used to induce EV production [41]. In the current study, bortezomib has been found to change the MMC-EV characteristics, decreasing the content of pro-angiogenic factors and increasing pro-inflammatory cytokines. Specifically, bortezomib has been found to significantly reduce the content of

the growth factors [VEGF-A, platelet-derived growth factor (PDGF) and angiogenin] in MMC-EVs. These growth factors are reported to regulate tumor-induced neo-angiogenesis in the BM of MM patients [42, 43] via activation of the signal transduction ERK1/2 and AKT [44–47].

We have observed that the uPAR level is increased in Bi-EVs. The interaction of uPAR with VEGFR-2 has been suggested to promote VEGF-induced angiogenesis [48]. One may assume that the increase in uPAR is part of the compensatory mechanism promoting the decrease in VEGFR-2 that we have found in Bi-EVs. We suggest that bortezomib inhibits angiogenesis by decreasing the pro-angiogenic potential of Bi-EVs.

Inflammatory cytokines released by MMCs have been shown to enhance plasma cell proliferation [49] and support MM progression [50]. Duality of inflammatory cytokine function has been previously reported. On the one hand, they are capable of inducing endothelial dysfunction [51], while on the other, they are found to promote angiogenesis through

EC activation of VEGF production [52], that together with IL-8 can support HUVEC migration [53].

Remarkably, while a suppressive mode of action of bortezomib in MM is well established, the results of the current study have exhibited negative effects of this drug on MMC-EVs exposed to this drug, which has actually up-regulated the expression of the tested inflammatory cytokines (interleukins IL1  $\beta$ , IL-8, and RANTES) in MMC-EVs. These findings are supported to some extent by the data from a recent study in mice, demonstrating that bortezomib has promoted pro-inflammatory macrophages, which could account for MMC aggressiveness [54]. Additionally, in another study, IL-8 has been reported to be associated with decreased effectiveness of proteasome inhibition [55]. Notably, the increased level of IL-10, an anti-inflammatory regulator, in Bi-EVs may indicate the acquirement of an escape mechanism by MMCs [56].

The migratory effect of MMC-EVs on ECs supports our assumption that these EVs play a substantial role in promoting angiogenesis, as recently suggested [22]. The impact of VEGF/VEGFR-2 signal transduction pathways (ERK1/2, JNK, and p38) on EC migration is well known [55, 57]. We have found that naïve MMC-EVs activate ERK1/2 and c-Jun phosphorylation but not that of MAPKAPK-2. These results comply with the migration capacity of ECs obtained in the presence of MAPKs inhibitors. Previous studies have demonstrated that bortezomib treatment had increased p38 and JNK expression in the MM RPMI8226 cell line [58] with no effect on p-ERK1/2 expression [58]. Our results, showing a reduction in the EC p-ERK1/2 level following co-culture with Bi-EVs, may suggest the existence of an additional action pathway of bortezomib on EC p-ERK1/2 that is mediated indirectly through EVs.

High proteasome activity is one of the MM hallmarks and the ubiquitin–proteasome pathway is critical for MMC growth and survival, which explains their sensitivity to bortezomib [59]. We have found that MMC-EVs contain functionally active proteasome and that the exposure of MMCs to bortezomib diminishes the proteasome activity in the generated EVs. Furthermore, ECs subjected to these EVs also exhibit reduced proteasome activity, which may reflect indirect bortezomib influence.

Of note, despite the fact that we have failed to find any residues of bortezomib in EVs, using HPLC method, we still cannot draw a definitive conclusion that the inhibitory effects of these EVs are not related at least in part to residual presence of very low concentrations of this drug.

The present study has several limitations. Only one MM cell line and one PI inhibitor used at a high dose (100 nM) known as apoptotic have been evaluated. The recommended bortezomib dose for the treatment of MM patients is 1.3–1.5 mg/m<sup>2</sup>. The study on blood distribution of bortezomib and its kinetics in MM patients found that the drug

concentration in whole blood and blood cells was much higher than that measured in plasma, differing between treatment cycles and remaining in the blood above 11 days after finalizing the treatment [60]. In the current study, the effects of EVs derived from MMCs pre-exposed to bortezomib have been assessed in an in-vitro model and the high dose of the drug was used to ensure the achievement of an apoptotic-activity [23]. Moreover, MMC cells were treated with 100 nM of bortezomib for 24 h only once. This cannot reflect a long-term treatment taking place in the clinical setting. One may assume that a long exposure to bortezomib could further enhance generation of EVs and intensify their effects.

In conclusion, this study has demonstrated that naïve MMC-EVs contain pro-angiogenic factors and enhance EC migration and proliferation. High bortezomib doses have induced apoptosis of MMCs resulting in generation of EVs differing from their naïve counterparts in size and content. These EVs have been found to limit EC functioning via specific signal transduction pathways and thus interfere with angiogenesis.

**Acknowledgements** We would like to thank Mrs. Sonia Kamenetsky for assistance in the preparation of this manuscript.

**Funding** This study was funded by the Israel Cancer Association (Grant Number 20120100) and by the Israel myeloma association (AMEN).

## Compliance with ethical standards

**Informed consent** Informed consent was obtained from all individual participants included in the study.

## References

- Ria R, Vacca A, Russo F, Cirulli T, Massaia M, Tosi P et al (2004) A VEGF-dependent autocrine loop mediates proliferation and capillarogenesis in bone marrow endothelial cells of patients with multiple myeloma. *Thromb Haemost* 92:1438–1445
- Roccaro AM, Sacco A, Maiso P, Azab AK, Tai YT, Reagan M et al (2013) BM mesenchymal stromal cell-derived exosomes facilitate multiple myeloma progression. *J Clin Invest* 123:1542–1555
- Xu S, Menu E, De Becker A, Van Camp B, Vanderkerken K, Van Riet I (2012) Bone marrow-derived mesenchymal stromal cells are attracted by multiple myeloma cell-produced chemokine CCL25 and favor myeloma cell growth in vitro and in vivo. *Stem Cells* 30:266–279
- Manier S, Sacco A, Leleu X, Ghobrial IM, Roccaro AM (2012) Bone marrow microenvironment in multiple myeloma progression. *J Biomed Biotechnol* 2012:157496
- Bergers G, Benjamin LE (2003) Tumorigenesis and the angiogenic switch. *Nat Rev Cancer* 3:401–410
- Ntellas P, Perivoliotis K, Dadouli K, Koukoulis GK, Ioannou M (2017) Microvessel density as a surrogate prognostic marker in patients with multiple myeloma: a meta-analysis. *Acta Haematol* 138:77–84

7. Shibuya M (2011) Vascular endothelial growth factor (VEGF) and its receptor (VEGFR) signaling in angiogenesis: a crucial target for anti- and pro-angiogenic therapies. *Genes Cancer* 2:1097–1105
8. Podar K, Tonon G, Sattler M, Tai YT, Legoull S, Yasui H et al (2006) The small-molecule VEGF receptor inhibitor pazopanib (GW786034B) targets both tumor and endothelial cells in multiple myeloma. *Proc Natl Acad Sci USA* 103:19478–19483
9. Tu Y, Chen C, Pan J, Xu J, Zhou ZG, Wang CY (2012) The Ubiquitin Proteasome Pathway (UPP) in the regulation of cell cycle control and DNA damage repair and its implication in tumorigenesis. *Int J Clin Exp Pathol* 5:726–738
10. Juvekar A, Manna S, Ramaswami S, Chang TP, Vu HY, Ghosh CC et al (2011) Bortezomib induces nuclear translocation of I $\kappa$ B $\alpha$  resulting in gene-specific suppression of NF- $\kappa$ B-dependent transcription and induction of apoptosis in CTCL. *Mol Cancer Res* 9:183–194
11. Pei XY, Dai Y, Grant S (2003) The proteasome inhibitor bortezomib promotes mitochondrial injury and apoptosis induced by the small molecule Bcl-2 inhibitor HA14-1 in multiple myeloma cells. *Leukemia* 17:2036–2045
12. Kubiczko L, Pour L, Sedlarikova L, Hajek R, Sevcikova S (2014) Proteasome inhibitors—molecular basis and current perspectives in multiple myeloma. *J Cell Mol Med* 18:947–961
13. Lynch C, Panagopoulou M, Gregory CD (2017) Extracellular vesicles arising from apoptotic cells in tumors: roles in cancer pathogenesis and potential clinical applications. *Front Immunol* 8:1174
14. Choi D, Lee TH, Spinelli C, Chennakrishnaiah S, D'Asti E, Rak J (2017) Extracellular vesicle communication pathways as regulatory targets of oncogenic transformation. *Semin Cell Dev Biol* 67:11–22
15. Feng Q, Zhang C, Lum D, Druso JE, Blank B, Wilson KF et al (2017) A class of extracellular vesicles from breast cancer cells activates VEGF receptors and tumour angiogenesis. *Nat Commun* 8:14450
16. Huang Z, Feng Y (2017) Exosomes derived from hypoxic colorectal cancer cells promote angiogenesis through Wnt4-induced beta-catenin signaling in endothelial cells. *Oncol Res* 25:651–661
17. Vader P, Breakefield XO, Wood MJ (2014) Extracellular vesicles: emerging targets for cancer therapy. *Trends Mol Med* 20:385–393
18. Gyorgy B, Szabo TG, Pasztoi M, Pal Z, Misjak P, Aradi B et al (2011) Membrane vesicles, current state-of-the-art: emerging role of extracellular vesicles. *Cell Mol Life Sci* 68:2667–2688
19. Tzorani I, Rebibo-Sabbah A, Brenner B, Aharon A (2015) Disease dynamics in patients with acute myeloid leukemia: new biomarkers. *Exp Hematol* 43:936–943
20. Aharon A, Sabbah A, Ben-Shaul S, Berkovich H, Loven D, Brenner B et al (2017) Chemotherapy administration to breast cancer patients affects extracellular vesicles thrombogenicity and function. *Oncotarget* 8:63265–63280
21. Arendt BK, Walters DK, Wu X, Tschumper RC, Jelinek DF (2014) Multiple myeloma cell-derived microvesicles are enriched in CD147 expression and enhance tumor cell proliferation. *Oncotarget* 5:5686–5699
22. Liu Y, Zhu XJ, Zeng C, Wu PH, Wang HX, Chen ZC et al (2014) Microvesicles secreted from human multiple myeloma cells promote angiogenesis. *Acta Pharmacol Sin* 35:230–238
23. Hideshima T, Richardson P, Chauhan D, Palombella VJ, Elliott PJ, Adams J et al (2001) The proteasome inhibitor PS-341 inhibits growth, induces apoptosis, and overcomes drug resistance in human multiple myeloma cells. *Cancer Res* 61:3071–3076
24. Aharon A, Brenner B, Katz T, Miyagi Y, Lanir N (2004) Tissue factor and tissue factor pathway inhibitor levels in trophoblast cells: implications for placental hemostasis. *Thromb Haemost* 92:776–786
25. Aharon A, Tamari T, Brenner B (2008) Monocyte-derived micro-particles and exosomes induce procoagulant and apoptotic effects on endothelial cells. *Thromb Haemost* 100:878–885
26. Liao H, He H, Chen Y, Zeng F, Huang J, Wu L (2014) Effects of long-term serial cell passaging on cell spreading, migration, and cell-surface ultrastructures of cultured vascular endothelial cells. *Cytotechnology* 66:229–238
27. Katzenell S, Shomer E, Zipori Y, Zylberfisz A, Brenner B, Aharon A (2012) Characterization of negatively charged phospholipids and cell origin of microparticles in women with gestational vascular complications. *Thromb Res* 130:479–484
28. Bochmann I, Ebstein F, Lehmann A, Wohlschlaeger J, Sixt SU, Kloetzel PM et al (2014) T lymphocytes export proteasomes by way of microparticles: a possible mechanism for generation of extracellular proteasomes. *J Cell Mol Med* 18:59–68
29. Wang J, De Veirman K, Faict S, Frassanito MA, Ribatti D, Vacca A et al (2016) Multiple myeloma exosomes establish a favourable bone marrow microenvironment with enhanced angiogenesis and immunosuppression. *J Pathol* 239:162–173
30. Mohan M, Marin A, Davies FE (2017) Update on the optimal use of bortezomib in the treatment of multiple myeloma. *Cancer Manag Res* 9:51–63
31. Jung L, Holle L, Dalton WS (2004) Discovery, development, and clinical applications of bortezomib. *Oncology* 18:4–13
32. Crescitelli R, Lasser C, Szabo TG, Kittel A, Eldh M, Dianzani I et al (2013) Distinct RNA profiles in subpopulations of extracellular vesicles: apoptotic bodies, microvesicles and exosomes. *J Extracell Vesicles*. <https://doi.org/10.3402/jev.v2i0.20677>
33. Koifman N, Biran I, Aharon A, Brenner B, Talmon Y (2017) A direct-imaging cryo-EM study of shedding extracellular vesicles from leukemic monocytes. *J Struct Biol* 198:177–185
34. Lasser C, Jang SC, Lotvall J (2018) Subpopulations of extracellular vesicles and their therapeutic potential. *Mol Aspects Med* 60:1–14
35. Neumann B, Klippert A, Raue K, Sopper S, Stahl-Hennig C (2015) Characterization of B and plasma cells in blood, bone marrow, and secondary lymphoid organs of rhesus macaques by multicolor flow cytometry. *J Leukoc Biol* 97:19–30
36. Turturici G, Tinnirello R, Sconzo G, Geraci F (2014) Extracellular membrane vesicles as a mechanism of cell-to-cell communication: advantages and disadvantages. *Am J Physiol Cell Physiol* 306:C621–C633
37. Martin RK, Brooks KB, Henningsson F, Heyman B, Conrad DH (2014) Antigen transfer from exosomes to dendritic cells as an explanation for the immune enhancement seen by IgE immune complexes. *PLoS ONE* 9:e110609
38. Kahn R, Mossberg M, Stahl AL, Johansson K, Lopatko Lindman I, Heijl C et al (2017) Microvesicle transfer of kinin B1-receptors is a novel inflammatory mechanism in vasculitis. *Kidney Int* 91:96–105
39. Di Raimondo F, Azzaro MP, Palumbo G, Bagnato S, Giustolisi G, Florida P et al (2000) Angiogenic factors in multiple myeloma: higher levels in bone marrow than in peripheral blood. *Haematologica* 85:800–805
40. Kumar S, Rajkumar SV, Greipp PR, Witzig TE (2004) Cell proliferation of myeloma plasma cells: comparison of the blood and marrow compartments. *Am J Hematol* 77:7–11
41. Todorova D, Simoncini S, Lacroix R, Sabatier F, Dignat-George F (2017) Extracellular vesicles in angiogenesis. *Circ Res* 120:1658–1673
42. Li XM, Zhang LP, Wang YZ, Lu AD, Chang Y, Zhu HH et al (2016) CD38+ CD58– is an independent adverse prognostic factor in paediatric Philadelphia chromosome negative B cell acute lymphoblastic leukaemia patients. *Leuk Res* 43:33–38
43. Tsirakis G, Pappa CA, Kanellou P, Stratinaki MA, Xekalou A, Psarakis FE et al (2012) Role of platelet-derived growth factor-AB

- in tumour growth and angiogenesis in relation with other angiogenic cytokines in multiple myeloma. *Hematol Oncol* 30:131–136
44. Coluccia AM, Cirulli T, Neri P, Mangieri D, Colanardi MC, Gnoni A et al (2008) Validation of PDGFRbeta and c-Src tyrosine kinases as tumor/vessel targets in patients with multiple myeloma: preclinical efficacy of the novel, orally available inhibitor dasatinib. *Blood* 112:1346–1356
  45. Miyake M, Goodison S, Lawton A, Gomes-Giacoa E, Rosser CJ (2015) Angiogenin promotes tumoral growth and angiogenesis by regulating matrix metalloproteinase-2 expression via the ERK1/2 pathway. *Oncogene* 34:890–901
  46. Alexandrakis MG, Passam FH, Sfridaki A, Kyriakou DS, Petreli E, Roussou P (2003) Elevated serum angiogenin in multiple myeloma. *Hematol J* 4:454–455
  47. Pappa CA, Tsirakis G, Boula A, Sfridaki A, Psarakis FE, Alexandrakis MG et al (2013) The significance of non correlation between interleukin-8 serum levels with bone marrow microvascular density in patients with myeloma multiple. *Pathol Oncol Res* 19:539–543
  48. Herkenne S, Paques C, Nivelles O, Lion M, Bajou K, Pollenus T et al (2015) The interaction of uPAR with VEGFR2 promotes VEGF-induced angiogenesis. *Sci Signal* 8:ra117
  49. Kovacs E (2010) Interleukin-6 leads to interleukin-10 production in several human multiple myeloma cell lines. Does interleukin-10 enhance the proliferation of these cells? *Leuk Res* 34:912–916
  50. Menu E, De Leenheer E, De Raeve H, Coulton L, Imanishi T, Miyashita K et al (2006) Role of CCR1 and CCR5 in homing and growth of multiple myeloma and in the development of osteolytic lesions: a study in the 5TMM model. *Clin Exp Metastasis* 23:291–300
  51. Bhagat K, Vallance P (1997) Inflammatory cytokines impair endothelium-dependent dilatation in human veins in vivo. *Circulation* 96:3042–3047
  52. Carmi Y, Dotan S, Rider P, Kaplanov I, White MR, Baron R et al (2013) The role of IL-1beta in the early tumor cell-induced angiogenic response. *J Immunol* 190:3500–3509
  53. Ju L, Zhou Z, Jiang B, Lou Y, Guo X (2017) Autocrine VEGF and IL-8 promote migration via Src/Vav2/Rac1/PAK1 signaling in human umbilical vein endothelial cells. *Cell Physiol Biochem* 41: 1346–1359
  54. Beyar-Katz O, Magidey K, Ben-Tsedek N, Alishekevitz D, Timaner M, Miller V et al (2016) Bortezomib-induced pro-inflammatory macrophages as a potential factor limiting anti-tumour efficacy. *J Pathol* 239:262–273
  55. Singha B, Gatla HR, Manna S, Chang TP, Sanacora S, Poltoratsky V et al (2014) Proteasome inhibition increases recruitment of IkkappaB kinase beta (IKKbeta), S536P-p65, and transcription factor EGR1 to interleukin-8 (IL-8) promoter, resulting in increased IL-8 production in ovarian cancer cells. *J Biol Chem* 289:2687–2700
  56. Alotaibi MR, Hassan ZK, Al-Rejaie SS, Alshammari MA, Almutairi MM, Alhoshani AR et al (2018) Characterization of apoptosis in a breast cancer cell line after IL-10 silencing. *Asian Pac J Cancer Prev (APJCP)* 19:777–783
  57. Gupta K, Kshirsagar S, Li W, Gui L, Ramakrishnan S, Gupta P et al (1999) VEGF prevents apoptosis of human microvascular endothelial cells via opposing effects on MAPK/ERK and SAPK/JNK signaling. *Exp Cell Res* 247:495–504
  58. Wen J, Feng Y, Huang W, Chen H, Liao B, Rice L et al (2010) Enhanced antimyeloma cytotoxicity by the combination of arsenic trioxide and bortezomib is further potentiated by p38 MAPK inhibition. *Leuk Res* 34:85–92
  59. Edwards CM, Lwin ST, Fowler JA, Oyajobi BO, Zhuang J, Bates AL et al (2009) Myeloma cells exhibit an increase in proteasome activity and an enhanced response to proteasome inhibition in the bone marrow microenvironment in vivo. *Am J Hematol* 84:268–272
  60. Osawa T, Naito T, Kaneko T, Mino Y, Ohnishi K, Yamada H et al (2014) Blood distribution of bortezomib and its kinetics in multiple myeloma patients. *Clin Biochem* 47:54–59